

Computer Simulation of Homopolymer and Copolymer Adsorption Dynamics

J. Scott Shaffer

Department of Chemical Engineering, University of Southern California,
Los Angeles, California 90089-1211

Received December 12, 1993; Revised Manuscript Received March 1, 1994*

ABSTRACT: We report computer simulations of single-chain polymer adsorption dynamics. The time required for adsorption is obtained as a function of the chain length and chemical composition of homopolymers, diblock copolymers, and random copolymers. The copolymers are composed of type A segments that adsorb strongly ($10 k_B T$ per segment) and type B segments that have no attractive interactions with the surface; homopolymers are composed exclusively of type A segments. A relaxation function for adsorption is defined as a normalized number of adsorbed segments; it is calculated by averaging over hundreds of statistically independent adsorption trials. Relaxation is nonexponential at short times, while at intermediate times the relaxation is described by a single time constant. At the longest times, a few long-lived nonequilibrium states are observed, and the relaxation is again nonexponential. A relaxation time for adsorption is defined as the time constant for the relaxation in the intermediate region. This relaxation time varies with the chain length of homopolymers according to a power law, with an exponent equal to 1.50 ± 0.04 when excluded volume interactions are ignored and 1.58 ± 0.04 when excluded volume interactions are enforced. For diblock copolymers, the adsorption time of single chains is almost independent of the nonadsorbing (type B) block length. For random copolymers with a fixed number of adsorbing segments, the chain length scaling of the adsorption time is similar to the scaling of the relaxation time of the end-to-end vector autocorrelation function in free and tethered chains.

1. Introduction

Polymer-solid interfaces are present in a number of technologically important material systems, including composite materials, adhesives, and colloidal dispersions. The widespread use of adsorbed polymers has motivated extensive study of these systems through theory, computer simulation, and experiment. As a result, the structural properties of adsorbed polymers at equilibrium are now fairly well understood.¹⁻⁴ Many questions remain, however, about the important subject of polymer adsorption dynamics. First, several experimental⁵⁻⁹ and theoretical¹⁰⁻¹⁵ studies suggest that adsorbed polymer layers form long-lived nonequilibrium states. It is presently difficult to characterize the structure of these nonequilibrium adsorbed layers, because their structure depends strongly on the details of the kinetic pathways that are available during adsorption. Second, many commercially relevant polymer-solid interfaces are composed of several surface-active polymeric species that may differ in chain length, surface affinity, chain architecture, and chemical composition. Given that adsorbed polymer layers have very long structural relaxation times, the interfacial structure in a mixture of several species may be kinetically, rather than thermodynamically, controlled. In other words, surface-active species that are thermodynamically favored at the interface may never reach their equilibrium adsorbed configurations if other species adsorb more rapidly during the fabrication process. Therefore, it is important to obtain general relationships or scaling laws that describe the dependence of polymer adsorption kinetics on chain length and chemical composition. Once these scaling laws are known, they can be used to assess the effects of processing conditions on the structure of nonequilibrium adsorbed layers, to judge whether a given interfacial structure is thermodynamically or kinetically controlled and to optimize the fabrication of polymer-solid interfaces.

The procedures used to fabricate polymer-solid interfaces involve many dynamical processes. Adsorption from

solution, for example, requires mass transport from the bulk polymer solution to the interfacial region, adsorption of individual chains onto the solid surface, buildup of the adsorbed polymer layer, and, ultimately, relaxation toward equilibrium.¹⁶ The present study addresses only one of the processes listed above: the adsorption of single polymer chains from a good solvent onto a flat, solid surface. We study the adsorption dynamics of homopolymers and obtain the scaling relationship between the adsorption time and the chain length. We also conduct simulations of the adsorption of diblock and random copolymers in order to study the effects of copolymer composition on adsorption dynamics.

The structural properties of isolated adsorbed homopolymers have been studied thoroughly by Monte Carlo simulations,¹⁷⁻¹⁹ Brownian dynamics,²⁰ and analytical theories.^{21,22} The equilibrium adsorption of a certain class of random copolymers (those with only a few strongly adsorbing segments) has been treated theoretically,²³ and lattice-based Monte Carlo simulations of copolymer structure at solid surfaces have recently appeared.^{24,25} In contrast, however, only a few theoretical or computational studies of the dynamical properties of dilute adsorbed polymers have been reported. Poland²⁶ has formulated a kinetic theory for adsorption of short chains; Hahn and Kovac²⁷ have performed Monte Carlo simulations of a tethered, but otherwise nonadsorbing chain on an FCC lattice; Konstadinidis et al.²⁸ have characterized the distribution of loops and tails that remain after a dynamic simulation of irreversible adsorption; and Cosgrove et al.^{29,30} have used Monte Carlo simulations of single chains on cubic lattices to look qualitatively at the dynamics of adsorption in weakly and strongly adsorbing regimes.

The present study differs from the ones cited above in several respects. First, we focus directly on the dynamics of adsorption from dilute solution by defining a relaxation function in terms of the evolution of the number of adsorbed segments. From the relaxation function, we extract a relaxation time for adsorption and establish scaling laws for the dependence of the relaxation time on

* Abstract published in *Advance ACS Abstracts*, April 15, 1994.

chain length and copolymer composition. Second, many of the previous studies have been concerned with tethered chains. Here we simulate the adsorption of chains that begin in a configuration that would result from mass transport from bulk solution to the surface; segments in the middle of the chain are often the first to adsorb. Third, we allow the adsorbed polymer segments to diffuse in the plane of the surface. Surface diffusion is expected to be an important contribution to the overall mobility of a partially adsorbed polymer. On metal surfaces, for example, the activation energy for surface diffusion of physisorbed alkanes is typically only a small fraction of the adsorption energy.³¹ In fact, molecular dynamics simulations of alkanes adsorbed on transition metal surfaces have shown that the adsorbed molecules retain a large amount of translational freedom.^{32,33}

2. Computational Method

2.1. Bond Fluctuation Model. The most realistic and detailed theoretical description of polymer adsorption dynamics would be one provided by molecular dynamics (MD) simulations of polymer chains in a solvent near an attractive surface. However, polymer adsorption occurs on time scales beyond those that are currently accessible to MD simulations. For example, polymer chains as short as eight repeat units require more than 10^{-10} s to adsorb when the segment-surface interaction energy is approximately $10 k_B T$;^{12,15} full MD simulations of longer chains are not computationally feasible. Another computational consideration arises because polymer adsorption is a nonequilibrium phenomenon. To accumulate appropriate nonequilibrium averages, simulations must be performed for many independent initial conditions. Since many simulations must be performed over very long time scales, the polymer adsorption dynamics must be described by a coarse-grained model that uses a reduced level of detail. Dynamic Monte Carlo simulations of polymer chains on lattices³⁴ are one suitable class of coarse-grained models.

In the present study, the polymer structure and dynamics are represented by the three-dimensional (3-D) bond fluctuation model (BFM), originally developed for bulk systems by Deutsch and Binder.³⁵ This model is a variant of a two-dimensional (2-D) fluctuating bond model introduced by Carmesin and Kremer.³⁶ In the 3-D BFM, polymer segments occupy eight neighboring sites that form a cube on a simple cubic lattice.³⁷ The excluded volume condition can be enforced by forbidding double occupancy of lattice sites. Bonded polymer segments are connected by bond vectors, $\mathbf{b} = (b_x, b_y, b_z)$, that run between the centers of the cubes that define the locations of the polymer segments. A unique feature of the BFM is that the lengths of the bond vectors can take several values.^{35,36} By allowing the bond lengths to fluctuate, the polymer chain configurations can evolve through local displacements of single polymer segments and still maintain chain connectivity. In the implementation of the BFM used here, each move in the Monte Carlo simulation involves a trial displacement of a polymer segment chosen at random by one lattice unit in a randomly chosen direction. In other words, the displacement vector, $\Delta\mathbf{b}$, satisfies

$$\Delta\mathbf{b} \in P(1,0,0) \quad (1)$$

where $P(x,y,z)$ denotes the set of all distinct permutations and inversions of the triplet (x,y,z) . For example,

$$P(1,0,0) = \{(1,0,0), (0,1,0), (0,0,1), (-1,0,0), (0,-1,0), (0,0,-1)\} \quad (2)$$

The displacement of a given segment during a trial move changes the bond vectors between the moving segment and its bonded neighbors along the chain. The Monte Carlo moves are accepted only if the new bond vectors are members of the set

$$P(2,0,0) \cup P(2,1,0) \cup P(2,1,1) \cup P(2,2,1) \cup P(3,0,0) \cup P(3,1,0) \quad (3)$$

When excluded volume interactions are enforced and the trial displacements satisfy eq 1, the bond vector restrictions given in eq 3 ensure that the polymer chain cannot pass through itself.³⁵ The BFM therefore accounts for both excluded volume and entanglement constraints in a computationally efficient manner. Note, however, that the model does not account for hydrodynamic interactions.³⁸

The 2-D and 3-D bond fluctuation models have been used extensively in simulations of polymer dynamics.³⁹⁻⁴¹ The success of these models in describing flexible polymers has come from the degree of realism that is incorporated in the models despite the artificial imposition of a lattice. As noted by the original authors,^{35,36} the fluctuations in the lengths of the bond vectors correspond to the natural fluctuations in the Kuhn segment length of real polymers. Another advantage of the BFM is the high effective coordination number of the lattice: each bond vector has 108 possible orientations in the 3-D BFM, in contrast to 6 orientations for bond vectors of unit length on a simple cubic lattice. The high coordination and the flexibility of bond vectors allow for the generation of new configurations in the middle of the polymer chain. As a result, the BFM is ergodic.⁴² It also avoids problems that can arise for self-avoiding chains in lattice Monte Carlo models that maintain constant bond lengths.^{43,44}

In the absence of a surface, a dynamic Monte Carlo (DMC) simulation of a free polymer with N segments proceeds as follows: (1) a polymer segment and trial displacement are chosen at random; (2) a test is performed to see if the excluded volume and bond vector constraints are satisfied; (3) if the constraints are not satisfied, the move is rejected; (4) if the constraints are satisfied, the move is accepted. The simulation clock is updated by one unit after N moves have been attempted. Therefore, the fundamental unit of simulation time is one Monte Carlo pass (MCP), which consists of N attempted moves of individual polymer segments. On average, then, each segment of the polymer chain is subject to one trial displacement per Monte Carlo pass. For simulations of isolated polymers, the BFM reproduces Rouse dynamical scaling:³⁶

$$D \sim N^{-1} \quad (4)$$

$$\tau_R \sim (N-1)^{\alpha_R} \quad (5)$$

where D is the self-diffusion coefficient and τ_R is the relaxation time of the end-to-end vector autocorrelation function (the rotational relaxation time).³⁸ The scaling exponent for τ_R is given by

$$\alpha_R = 1 + 2\nu \quad (6)$$

where ν is the scaling exponent of the mean-square end-to-end distance. For polymers in three dimensions, $\nu = 1/2$ in the absence of excluded volume interactions, and $\nu \approx 0.588$ when excluded volume interactions are present.⁴⁵

2.2. Surface Model. An impenetrable, flat surface is easily introduced into the BFM by placing a hard wall at

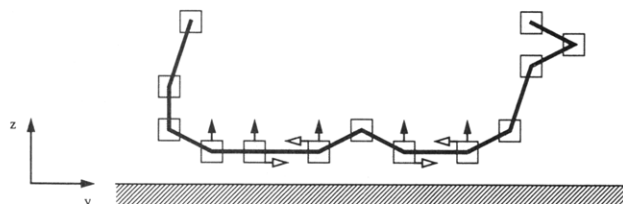


Figure 1. Two-dimensional schematic view of an adsorbed polymer as it is represented in the three-dimensional bond fluctuation model. The view is parallel to the surface, along the x axis. Polymer segments are represented by the shaded squares, although of course they are actually cubes on a three-dimensional lattice. Bonds between segments are represented by the dark line segments. For clarity, the underlying lattice is not shown. Open arrows denote attempted Monte Carlo moves that correspond to surface diffusion and are acceptable based on the excluded volume and bond length restrictions; these moves would be subject to an activation barrier of E_{xy} . Filled arrows denote attempted Monte Carlo moves that correspond to desorption and are acceptable based on the excluded volume and bond length restrictions; these moves would be subject to an activation barrier of E_z .

lattice plane $z = 0$. The polymer chain is confined to the half-space $z \geq 1$, and polymer segments in lattice plane $z = 1$ are considered to be adsorbed. The polymer-surface interactions are modeled by introducing activation energies for the motion of adsorbed segments. In general, we can impose an activation barrier E_{xy} for motion that corresponds to surface diffusion and an activation barrier E_z for motion that corresponds to desorption. A schematic view of an adsorbed polymer modeled by the BFM is presented in Figure 1.

In the presence of a surface, each Monte Carlo move proceeds as follows: (1) a polymer segment and trial displacement are chosen at random; (2) a test is performed to see if the excluded volume and bond vector constraints are satisfied; (3) if the constraints are not satisfied, the move is rejected; (4) if the constraints are satisfied and the segment was not adsorbed prior to the attempted move, the move is accepted; (5) if the constraints are satisfied and the attempted move is a displacement parallel to the surface in lattice plane $z = 1$ (surface diffusion), the move is accepted with probability $p = \exp(-E_{xy}/k_B T)$; (6) if the constraints are satisfied and the attempted move is a displacement from lattice plane $z = 1$ to $z = 2$ (desorption), the move is accepted with probability $p = \exp(-E_z/k_B T)$; (7) if the attempted move is a displacement from lattice plane $z = 1$ to $z = 0$ (surface penetration), the move is rejected. As in simulations without a surface, the simulation clock is updated by one unit (one Monte Carlo pass) after N moves have been attempted. The activation energy for desorption, E_z , is equivalent to the adsorption energy per segment.⁴⁶ Therefore, $E_z/k_B T$ determines the number of adsorbed segments at equilibrium. The activation barrier for surface diffusion, $E_{xy}/k_B T$, affects adsorption dynamics, but not equilibrium properties.⁴⁷ Since the excluded volume interactions are athermal, temperature enters the simulations only through $E_{xy}/k_B T$ and $E_z/k_B T$.

For the homopolymers in the present study, each segment is made to adsorb strongly, with adsorption energy $E_z/k_B T = 10$. For comparison, the surface interaction parameter, χ_s , for poly(methyl methacrylate) (PMMA) adsorbing on oxidized silicon is approximately 4 at room temperature.⁷ Although precise values of E_{xy} for polymer-solid systems are difficult to obtain, the ratio of E_{xy}/E_z typically ranges from 0.1 to 0.3 for short alkanes adsorbed on metal surfaces.³¹ In preliminary studies, the value of the activation barrier for surface diffusion was varied from $E_{xy}/k_B T = 0$ to $E_{xy}/k_B T = 2$. The rate of adsorption decreased as E_{xy} increased, but the overall effect of E_{xy} on

Table 1. Simulation Parameters^a

| N | M | τ_{bulk} | L_{xy} | L_z | ρ_s |
|-----|------|----------------------|----------|-------|----------|
| 10 | 1000 | 1000 | 40 | 250 | 0.0250 |
| 20 | 500 | 5000 | 57 | 250 | 0.0246 |
| 30 | 333 | 10000 | 70 | 250 | 0.0245 |
| 40 | 250 | 25000 | 80 | 250 | 0.0250 |
| 50 | 200 | 40000 | 90 | 250 | 0.0247 |
| 60 | 167 | 60000 | 98 | 250 | 0.0250 |
| 80 | 125 | 100000 | 113 | 250 | 0.0251 |

^a N is the total number of segments, M is the number of independent adsorption trials, τ_{bulk} is the bulk equilibration time in units of Monte Carlo passes, L_{xy} and L_z are the simulation box lengths, and ρ_s is the surface density corresponding to a fully adsorbed homopolymer chain, as calculated by eq 8.

the adsorption dynamics was rather small. In sections 3 and 4, we present results only for $E_{xy}/k_B T = 0$. Lateral motion is probably much more restricted when adsorption occurs through hydrogen bonding, chemisorption, or a specific chemical interaction. A systematic exploration of the effects of the activation energies E_{xy} and E_z will be the subject of future work.

When treating copolymer adsorption, we distinguish between strongly adsorbing segments, labeled type A segments, for which $E_{xy}/k_B T = 0$ and $E_z/k_B T = 10$, and nonadsorbing segments, labeled type B, for which $E_{xy}/k_B T = 0$ and $E_z/k_B T = 0$. By comparison, the homopolymers are composed entirely of type A segments. We do not include any energetic interactions between the type A and B segments of the copolymers other than the excluded volume interaction; the segments differ only in their interactions with the surface. As a result, these copolymers would not exhibit any of the interesting bulk phase segregation phenomena that are observed in many real copolymers.⁴⁸⁻⁵⁰

2.3. Initial Configurations. Many statistically independent realizations of the adsorption process must be simulated in order to accumulate reliable measures of the adsorption dynamics. For each chain length, N , we simulate M independent adsorption trials so that the product $NM = 10000$. (Table 1 contains the simulation parameters for each chain length studied.) Statistically independent initial configurations for each chain length are generated as follows: First, a single chain is grown in a box of length $L = 100$ in which periodic boundary conditions are applied in all coordinate directions. (No surface is present.) The chain growth proceeds by picking a starting point at random, adding bond vectors chosen at random from the reduced set

$$P(2,0,0) \cup P(2,1,0) \cup P(2,1,1) \cup P(3,0,0) \quad (7)$$

and rejecting additions that violate the excluded volume condition. Using the reduced set of bond vectors in eq 7 instead of the full set given in eq 3 ensures that no bond crossings are present in the initial configuration.³⁹ When no bond crossings are present initially, the dynamic Monte Carlo rules that employ the full set of bond vectors ensure that no bond crossings will arise during the course of the dynamics.³⁵ After the free chain is grown randomly, it subject to the MC algorithm given in section 2.1 (with no surface present) for a period of $10 \tau_{\text{bulk}}$ Monte Carlo passes (MCP), where τ_{bulk} is a bulk "equilibration time" that is approximately equal to the rotational relaxation time, τ_R . (The values of τ_{bulk} for each chain length are given in Table 1.) During this equilibration time, the end-to-end distance, radius of gyration, and bond lengths assume their equilibrium values. After the equilibration period, the polymer chain is subject to the MC algorithm for a period of $M \tau_{\text{bulk}}$ MCP. The polymer configuration is recorded after each

interval of τ_{bulk} MCP. The M configurations that are generated are then used for the independent adsorption trials that are discussed below. The simulations of homopolymers, diblock copolymers, and random copolymers use the same sets of initial configurations; they differ only in the chemical identity assigned to the polymer segments.

2.4. Adsorption Trials. The simulations were performed for a single polymer chain within a simulation box of dimensions $L_{xy} \times L_{xy} \times L_z$. In all simulations reported here, $L_z = 250$. The adsorbing surface is present at $z = 0$. Another impenetrable surface is present at $z = L_z + 1$, but this upper surface does not affect the adsorption that occurs on the lower surface because L_z is much greater than any linear dimension of the polymer chains. (For example, the root mean square end-to-end distance $\langle R^2 \rangle^{1/2} = 35$ for $N = 80$.) Periodic boundary conditions are applied in the x and y directions. As the chain length varies, the surface density, ρ_S corresponding to a fully adsorbed chain is kept approximately constant by adjusting L_{xy} according to

$$\rho_S = 4N/L_{xy}^2 \quad (8)$$

The factor of four is included because each adsorbed polymer segment in the BFM covers four lattice sites on the surface. Table 1 lists the box sizes and surface densities for each chain length.

Each adsorption trial begins with a partially adsorbed polymer chain, so that we can focus on the adsorption process itself rather than the diffusion of chains from the bulk solution to the surface. The initial adsorbed configurations are generated as follows: One of the M free chains that has been obtained from the algorithm discussed in section 2.3 is translated (without changing its internal configuration) in the z direction until at least one of its segments is in lattice plane $z = 1$. (In some configurations, more than one segment is initially located at $z = 1$. King and Cosgrove³⁰ discuss how the number of initially adsorbed segments varies with chain length.) For the homopolymers, each segment is of type A and adsorbs strongly, so the translation operation results in a partially adsorbed polymer that defines the initial condition.

To generate partially adsorbed copolymers, the copolymer compositions must be chosen in accord with the initial configurations. For random copolymers, the first segment along the chain that is in lattice plane $z = 1$ is assigned the identity of type A, and then the remaining type A segments are assigned by picking segments at random and labeling them type A segments. This procedure produces "ideal" random copolymers in which the chemical identity of each segment is statistically independent of the identities of every other segment. However, the statistical properties of the random copolymers in the present study are not exactly the same as the properties of the polymers that are described in previous studies of random copolymer thermodynamics.^{49,50} In refs 49 and 50, the number of type A segments fluctuates from chain to chain around its average value, $p_A N$, where p_A is the probability of a given segment being of type A. Here, all random copolymers have exactly N_A adsorbing segments; there is no fluctuation from one adsorption trial to the next.

For diblock copolymers in which $N_A \geq N/2$, the segment types are assigned so that the adsorbing block of type A segments contains at least one of the segments in lattice plane $z = 1$.⁵¹ Diblock copolymers for which $N_A < N/2$ must be treated differently. If any segment that is in contact with the surface is in a position j along the chain, where $j \leq N_A$ or $j > N - N_A$, then we assign the adsorbing block to the end of the chain that will include a segment

in lattice plane $z = 1$. It is possible, however, that the only segments that are in contact with the surface are those with positions along the chain j , where $N_A < j \leq N - N_A$. In this case, neither assignment of the adsorbing block will include any segments initially in contact with the surface. We then translate the polymer back into the center of the box and execute the MC algorithm for free chains, given in section 2.1, until the polymer chain adopts a configuration in which the segment that is nearest to the surface (and will be in contact with the surface after the translation operation) is in a position j along the chain where $j \leq N_A$ or $j > N - N_A$. Following the translation, the segment assignments result in an adsorbing block in contact with the surface.

2.5. Relaxation Function and Relaxation Time. The generation of the initial partially adsorbed configuration and the assignment of the copolymer composition define the time origin, $t = 0$. The MC simulations then begin according to the algorithm described in section 2.2. As the simulations proceed, the number of adsorbed segments, $n(t)$, is monitored. (The number of adsorbed segments is defined as the number of type A segments that are in the lattice plane $z = 1$.) The adsorption dynamics are quantified by defining a relaxation function for adsorption, $q(t)$, as follows:

$$q(t) = \frac{n(t) - n_{\text{eq}}}{n(0) - n_{\text{eq}}} \quad (9)$$

where $n(t)$ is the number of segments adsorbed at time t , $n(0)$ is the number of segments adsorbed at time $t = 0$, and n_{eq} is the number of segments adsorbed at equilibrium. Since the type A segments adsorb strongly with $E_z/k_B T = 10$, n_{eq} is almost exactly equal to the number of type A segments; we take $n_{\text{eq}} = N$ for homopolymers and $n_{\text{eq}} = N_A$ for copolymers when calculating $q(t)$. The relaxation function is computed by averaging over the M independent adsorption trials. For homopolymers and diblock copolymers, the trials are made to be independent by using different initial configurations. For random copolymers, both the initial configuration and chemical sequence are independent from trial to trial.

A relaxation time can be defined in terms of the relaxation function in several ways. By performing the adsorption simulations and computing the relaxation function, we have found that $q(t)$ decays exponentially during most of the adsorption process. Thus, we define our relaxation time for adsorption, τ , as the time constant of the exponential decay of the relaxation function in the region $0.10 \leq q(t) \leq 0.50$. More precisely, the relaxation function is fit to the functional form

$$q(t) = c \exp(-t/\tau) \quad (10)$$

in the specified region, where exponential relaxation is always observed, and the relaxation time, τ , is taken from the best fit. Alternatively, the relaxation time could be defined by the time integral of the relaxation function:

$$\tau_{\text{alt}} = \int_0^\infty q(t) dt \quad (11)$$

where τ_{alt} denotes the alternative definition. If the decay of $q(t)$ is purely exponential over the entire time range, then the two definitions in eqs 10 and 11 are equivalent. The relaxation functions obtained from the simulations are not purely exponential however; instead, they contain long-time tails that are due primarily to a few long-lived partially desorbed states. We discuss the nature of these states in detail in section 3.2. For the purpose of defining

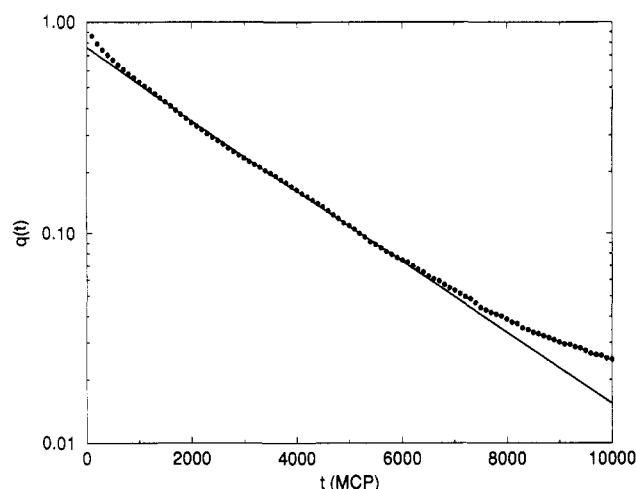


Figure 2. Semilogarithmic plot of the relaxation function, $q(t)$, defined by eq 9, for a homopolymer of chain length $N = 20$. The relaxation function was obtained by averaging over $M = 500$ independent adsorption trials. The time units are Monte Carlo passes (MCP). Filled circles are the data obtained from the simulations. The line is a fit to $q(t) = c \exp(-t/\tau)$ using the data in the region $0.10 \leq q(t) \leq 0.50$.

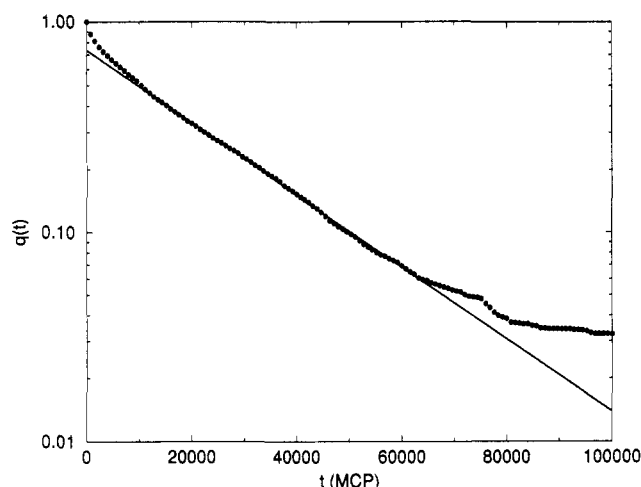


Figure 3. Same as Figure 2 for $N = 80$ and $M = 125$.

the relaxation time, we state here only that the lifetimes of these states may be artificially too large in the present lattice model, so allowing them to contribute significantly to the relaxation time seems to be unwarranted. The relaxation time, τ , that is obtained from eq 10 serves as a more robust quantitative measure of the relaxation dynamics.⁵²

3. Adsorption Dynamics: Homopolymers

In this section we present the results of the 3-D BFM simulations of homopolymer adsorption dynamics. Figures 2 and 3 show the relaxation function for the adsorption of homopolymers of length $N = 20$ and $N = 80$ in the form of a semilogarithmic plot. At short times when $q(t) > 0.50$, the relaxation is nonexponential. Although it is not shown in Figures 2 and 3, $q(t)$ can be represented in this region by a superposition of exponential functions. Over most of the adsorption period, when $0.05 \leq q(t) \leq 0.50$, the relaxation function can be described by a simple exponential decay. At long times, however, $q(t)$ begins to deviate from exponential decay, and the relaxation is much slower than predicted by the time constant describing the exponential region. We will return to the discussion of this long-time region in section 3.2.

3.1. Dynamical Scaling. The quality of a single-exponential description in the region $0.10 \leq q(t) \leq 0.50$

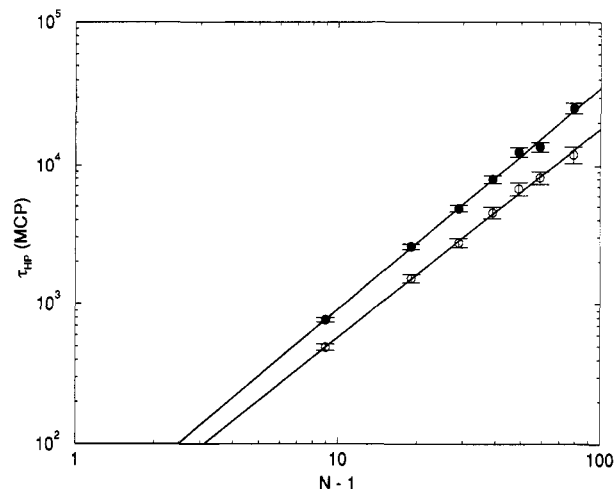


Figure 4. log-log plot of the adsorption time for homopolymers, τ_{HP} , in units of Monte Carlo passes (MCP), as a function of the number of bonds, $N - 1$. Open circles denote phantom chains with no intrachain excluded volume interactions; filled circles denote self-avoiding chains for which excluded volume interactions are enforced. In this figure and in Figures 6–10, the error bars indicate 95% confidence intervals. The two lines correspond to eq 12 with $\alpha = 1.50$ for the phantom chains and $\alpha = 1.58$ for the self-avoiding chains.

is illustrated by the solid lines through the simulation data in Figures 2 and 3. As discussed in section 2.5, we use the time constant of the exponential decay in this region to define the relaxation time for adsorption. The relaxation times that are generated from the simulation data have been used to obtain scaling laws for the dependence of the relaxation time on homopolymer chain length. Figure 4 presents a plot of the adsorption time, τ_{HP} , as a function of the number of bonds in the homopolymer, $N - 1$, for two cases: phantom chains with no intrachain excluded volume interactions and self-avoiding chains for which excluded volume interactions are enforced. (In both cases the set of allowed bond vectors is the same and is given by eq 3.) Also shown in Figure 4 are the best fits of the relaxation times to the power law

$$\tau_{HP} \sim (N - 1)^\alpha \quad (12)$$

Equation 12 describes the data very well over the region of chain lengths that have been studied; the power law exponents are $\alpha = 1.50 \pm 0.04$ for homopolymers without excluded volume and $\alpha = 1.58 \pm 0.04$ for homopolymers with excluded volume.^{53,54} The exponent $\alpha = 1.50 \pm 0.04$ for adsorption without excluded volume is suggestive of an exact scaling law, $\alpha = 3/2$, but we have not found any theoretical estimates of this quantity in the literature.

The simulation results show that the relaxation time for adsorption is a weaker function of chain length than the end-to-end vector relaxation time for free³⁸ and tethered²⁷ polymer chains. Hahn and Kovac²⁷ have found that end-to-end vector relaxation times for tethered chains, $\tau_{R,T}$, are approximately 3 times larger than those for free chains; however, the presence of an impenetrable surface does not change the scaling of the relaxation times with chain length. Hahn and Kovac obtain

$$\tau_{R,T} \sim (N - 1)^{\alpha_{R,T}} \quad (13)$$

with $\alpha_{R,T} = 1.95$ for tethered chains without excluded volume and $\alpha_{R,T} = 2.16$ for tethered chains with excluded volume.²⁷ These scaling exponents are consistent with those given by eqs 5 and 6 for free chains. A simple, but ultimately incorrect, scaling argument based on diffusive modes of motion suggests that the scaling of τ_{HP} with chain

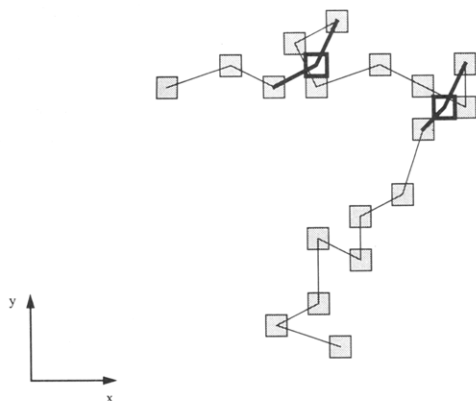


Figure 5. Illustration of a representative nonequilibrium configuration that persists for long times in a homopolymer with $N = 20$ segments. The view is along the z axis, looking down from above the surface. Shaded squares denote adsorbed segments in lattice plane $z = 1$. Thin lines represent bonds between adsorbed segments. Unshaded squares with bold outlines denote desorbed segments in lattice plane $z = 3$. Bold lines represent bonds between adsorbed segments and the desorbed segments. Both desorbed segments are immobile in the current configuration because of the excluded volume and bond vector restrictions.

length will also be consistent with eqs 5 and 6.⁵⁵ The exponents obtained from the simulations are $\alpha = 1.50$ and $\alpha = 1.58$, however. By comparing the true scaling exponents for τ_{HP} with those for τ_R and $\tau_{R,T}$, we conclude that the modes of relaxation that are important for the adsorption of homopolymers differ from those that are important for configurational relaxation in free polymers and tethered chains.

The difference between adsorption dynamics and configurational relaxation arises because the presence of an adsorbing surface disrupts the isotropic diffusive motion that is characteristic of the Rouse modes in the absence of a surface. (The adsorbing surface in the present work acts like a sink for the diffusing polymer segments rather than as a reflecting barrier as in the simulations of Hahn and Kovac.) It is certainly reasonable to find a weaker scaling for τ_{HP} than for τ_R and $\tau_{R,T}$. Each segment that adsorbs brings its bonded neighbors very close to the surface, and they then have a high probability of adsorbing in a short period of time. One intuitive picture that arises is of adsorption occurring by a "zippering" process, in which the segments adsorb sequentially once the first segment has arrived on the surface. The real adsorption dynamics must be more complicated, however, because a pure zippering process should give rise to an adsorption time that scales linearly with N . Processes like zippering do occur, however, in systems like PMMA adsorbing on aluminum, where strong and specific segment-surface interactions lead to highly cooperative dynamics.¹⁴

3.2. Nonequilibrium Configurations. Long-lived nonequilibrium configurations develop in a small fraction of the homopolymer adsorption trials that are conducted in the presence of excluded volume constraints. As Figures 2 and 3 suggest, several chains of length $N = 20$ and $N = 80$ remain in partially desorbed nonequilibrium states at times exceeding 10 000 MCP and 100 000 MCP, respectively. A typical nonequilibrium configuration is sketched in Figure 5 for a homopolymer with $N = 20$ segments. These nonequilibrium configurations usually involve one segment that hovers several lattice units above the surface in a region that is locally crowded with adsorbed segments. Due to the combination of excluded volume and bond vector restrictions, the two segments that remain desorbed in Figure 5 are completely immobile; their mobility can be restored only when their bonded neighbors desorb or

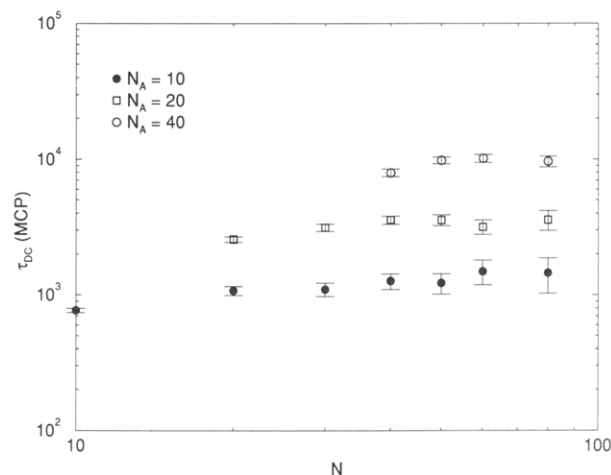


Figure 6. log-log plot of the adsorption time for diblock copolymers, τ_{DC} , as a function of total chain length, N , for several adsorbing block lengths, N_A .

their nonbonded neighbors diffuse out of the region below them. The rate of desorption of bonded neighbors is limited by the large activation barrier, E_z ; the surface diffusion of the other nearby segments is also suppressed because of the high local concentration of adsorbed segments and the bond vector restrictions that are imposed by the lattice representation. Since the BFM artificially discretizes segment positions and bond vectors, we believe that these particular structures within the BFM relax more slowly than real polymers or comparable structures in off-lattice simulations. In this respect, these nonequilibrium structures are artifacts of the lattice representation of the polymer structure and the particular rules that were chosen for the dynamic Monte Carlo simulation.⁵⁶ Nevertheless, these structures should be qualitatively representative of highly twisted and constrained configurations that will exist during the adsorption of flexible polymers. The primary difference is that real polymers can accommodate strain along the backbone bond and torsion angles in order to relax any twisted structures that form during the course of adsorption.

Even if these nonequilibrium structures are primarily due to the lattice representation, their quantitative effect on the relaxation function, $q(t)$, is very small, because only a small fraction of the initially adsorbed configurations evolve into nonequilibrium configurations like the one illustrated in Figure 5. Furthermore, the number of nonadsorbed segments in these structures is typically no more than 10% of the total number of segments. Thus, the nonequilibrium structures contribute to $q(t)$ only at long times when $q(t) < 0.05$. Therefore, the presence of these nonequilibrium configurations should not affect the relaxation times that are obtained from $q(t)$, because $q(t)$ is fit to an exponential decay in the intermediate time region where these highly constrained structures do not contribute significantly to the relaxation function.

4. Adsorption Dynamics: Copolymers

4.1. Diblock Copolymers. We turn now to discuss the adsorption of diblock copolymers for which excluded volume interactions are enforced. (Copolymers without excluded volume interactions were not studied.) Figure 6 shows the adsorption time for diblock copolymers, τ_{DC} , as a function of total chain length, N , for several values of the adsorbing block length, N_A . Conversely, Figure 7 shows τ_{DC} as a function of the number of bonds in the adsorbing block, $N_A - 1$, for several values of N . It is clear that the time required for the adsorption of these isolated diblock copolymers is determined predominantly by the

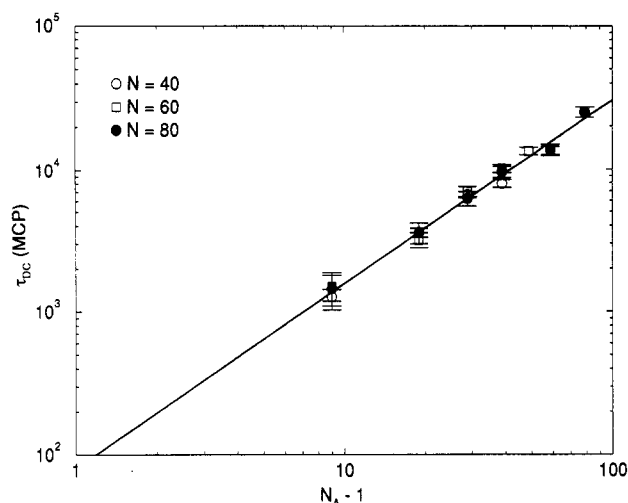


Figure 7. log-log plot of the adsorption time for diblock copolymers, τ_{DC} , as a function of the number of bonds in the adsorbing block, $N_A - 1$, for several total chain lengths, N . The line corresponds to eq 14 with $\beta = 1.29$.

length of the adsorbing block rather than the total chain length. The nonadsorbing block therefore must not impose a significant steric constraint to the adsorption of the adsorbing block. In Figure 6, for example, the relaxation times for diblock copolymers with adsorbing block lengths $N_A = 10$ increase less than a factor of 2 as the total chain length increases from $N = 10$ to $N = 80$. Nevertheless, the impact of the nonadsorbing block can be seen in the variation of τ_{DC} with N_A .

The dependence of τ_{DC} on N_A when N is fixed can be described as follows:

$$\tau_{DC} \sim (N_A - 1)^{\beta} \quad (14)$$

with $\beta = 1.29 \pm 0.10$.⁵³ This power law scaling over the range of chain lengths studied is shown in Figure 7. In comparison to the homopolymer dynamic scaling in eq 12, one might expect $\beta = \alpha$, since the nonadsorbing block has only a weak quantitative effect on the diblock adsorption when N_A is held fixed. The discrepancy between α and β arises, however, because the presence of the nonadsorbing block alters the conformational statistics of the adsorbing block. In other words, the structure of an adsorbing block with N_A segments in a self-avoiding copolymer of N total segments is not the same as the structure of a homopolymer with N_A segments. Specifically, the mean-square distance, $\langle R_{ij}^2 \rangle$, between two segments i and j in a self-avoiding chain depends on the total chain length, N , even when i and j are fixed.⁵⁷⁻⁵⁹ Furthermore, the scaling of $\langle R_{ij}^2 \rangle$ with $|i - j|$ is not simply $\langle R_{ij}^2 \rangle \sim |i - j|^{2\nu}$; instead, the scaling depends explicitly on N . The effects of the nonadsorbing block on the static properties of the diblock copolymers is then manifested in the dynamical scaling behavior as given by eq 14. A word of caution is in order, however. Since the static properties of the adsorbing blocks depend explicitly on the total chain length N , the scaling law coefficient β , which describes the variation of the adsorption time with N_A , may also depend explicitly on N . The range of chain lengths that has been studied is not large enough to evaluate the precise magnitude of the variation of β with N . As a result, the asymptotic value of the scaling exponent for eq 14 should be regarded as uncertain.

4.2. Random Copolymers. The adsorption of random copolymers is qualitatively different from the adsorption of homopolymers and diblocks. Figure 8 shows the adsorption time for random copolymers, τ_{RC} , as a function of the total number of bonds, $N - 1$, for several values of N_A ; Figure 9 shows τ_{RC} as a function of N_A for several

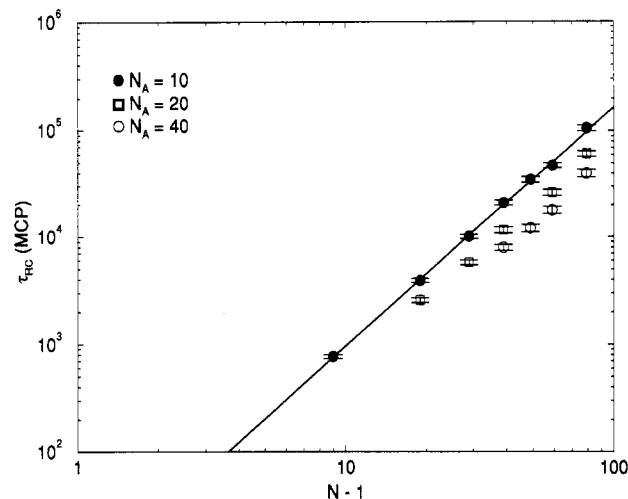


Figure 8. log-log plot of the adsorption time for random copolymers, τ_{RC} , as a function of total number of bonds, $N - 1$, for several numbers of adsorbing segments, N_A . The bold line through the data for $N_A = 10$ corresponds to eq 15 with $\gamma = 2.24$.

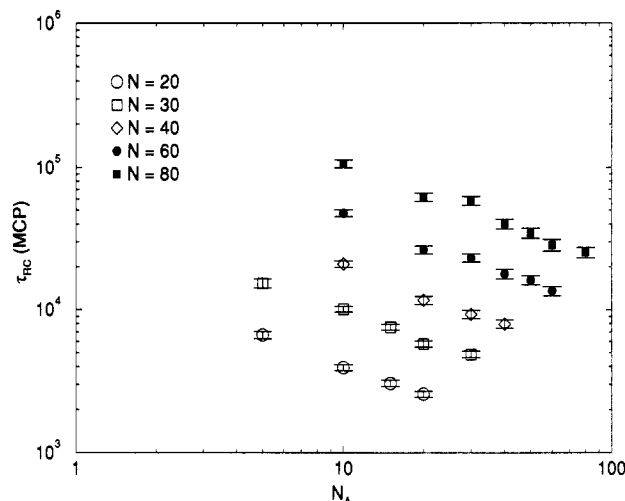


Figure 9. log-log plot of the adsorption time for random copolymers, τ_{RC} , as a function of the number of adsorbing segments, N_A , for several values of the total chain length, N .

values of N . In contrast to diblock copolymers, the adsorption time for random copolymers varies strongly with both N at constant N_A and with N_A at constant N . Perhaps a surprising result is that the relaxation times for adsorption at a fixed value of N actually decrease as N_A increases; even though more segments must adsorb, the adsorption proceeds more rapidly. Since random copolymers with large values of N_A will contain (on average) longer sequences of type A segments, a segment-by-segment adsorption mechanism (akin to "zippering") may be more important as the ratio N_A/N increases.⁶⁰

Random copolymers also differ from the other polymer architectures in their dynamical scaling during adsorption. The chain length dependence of τ_{RC} is much stronger than that of τ_{HP} or τ_{DC} . The solid line in Figure 8 represents an approximate power law scaling of τ_{RC} with $N - 1$ when N_A is fixed:

$$\tau_{RC} \sim (N - 1)^{\gamma} \quad (15)$$

with $\gamma = 2.24 \pm 0.04$ when $N_A = 10$.^{53,54} The exponent γ is greater than the exponents α and β from eqs 12 and 14 which describe the homopolymer and diblock copolymer scaling. Instead, γ is approximately equal to α_R and $\alpha_{R,T}$, the scaling exponents for the end-to-end vector relaxation time in free³⁸ and tethered²⁷ chains. This similarity between random copolymer adsorption dynamics and

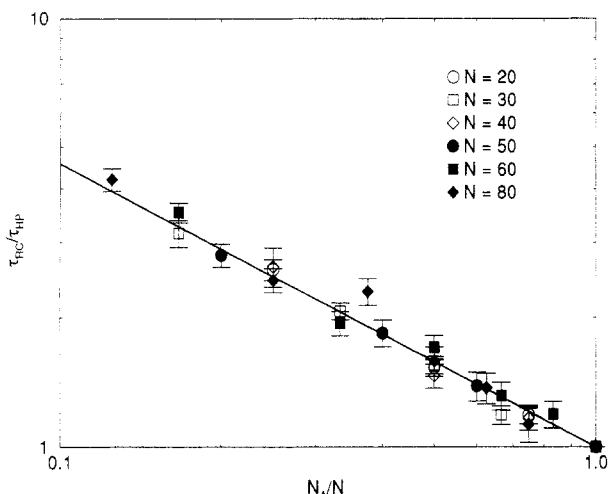


Figure 10. log-log plot of the ratio $\tau_{RC}(N_A, N)/\tau_{HP}(N)$ as a function of the fraction of adsorbing segments in the random copolymer, $f = N_A/N$. The line is the scaling law given by eq 16 with $\zeta = 0.66$.

configurational relaxation can be explained as follows. As N increases at constant N_A , the adsorbing segments become diluted along the chain backbone. For $N/N_A \gg 1$, the partially adsorbed random copolymers will consist of long tethered loops and tails in which each adsorbing segment is, on average, separated from the next adsorbing segment by N/N_A nonadsorbing segments. Considering the simulations of Hahn and Kovac,²⁷ it is reasonable to expect Rouse-like motion in these tethered subchains. The approach of the next adsorbing segment to the surface will then be limited by the diffusive motion of the loops and tails, and this is reflected in the similar scaling exponents for τ_R , $\tau_{R,T}$, and τ_{RC} .

Another scaling relationship can be obtained by considering the ratio of the adsorption time, $\tau_{RC}(N_A, N)$, of a random copolymer with N_A adsorbing segments and N total segments to the adsorption time of a homopolymer with the same total number of segments, $\tau_{HP}(N)$:

$$\frac{\tau_{RC}(N_A, N)}{\tau_{HP}(N)} \sim f^\zeta \quad (16)$$

where $f = N_A/N$ is the fraction of adsorbing segments. The exponent ζ can be obtained by considering a fixed value of N_A and combining the random copolymer scaling of eq 15 with the homopolymer scaling of eq 12. The result is $\zeta = \gamma - \alpha = 0.66$. As shown in Figure 10, the simulation data are consistent with this scaling law, although the quantity $\tau_{RC}(N_A, N)/\tau_{HP}(N)$ is scattered rather widely due to the statistical uncertainty in the values of both τ_{RC} and τ_{HP} that are obtained from the MC simulations.

5. Concluding Remarks

We have presented a computer simulation study of single-chain homopolymer and copolymer adsorption dynamics. The bond fluctuation lattice model of Deutsch and Binder³⁵ has been generalized to include an impenetrable surface with activation energies for surface diffusion and desorption, E_{xy} and E_z , respectively. In the present study, specific values of E_{xy} and E_z were chosen so that segments could adsorb strongly but retain translational freedom on the surface. For single diblock copolymers, the adsorption time is nearly independent of the length of the nonadsorbing block. The scaling relationships of eqs 12 and 15 describe the dependence of the adsorption times of single homopolymers and random copolymers on chain length and composition. We should

note, however, that the scaling exponents have been obtained in the absence of hydrodynamic interactions. As in the case of polymer dynamics in dilute solution, the inclusion of hydrodynamic interactions may change the value of the scaling exponents.³⁸ Near a surface, the effects of hydrodynamic interactions may be even more pronounced. Further work will also be required to examine adsorption dynamics in multichain systems at higher concentrations.

Even though the simulation results are limited to the initial stages of adsorption from dilute solution, they can be used to illustrate several nonequilibrium phenomena in polymer adsorption. For example, consider a dilute bidisperse mixture of homopolymers that differ in chain length by a factor of 3, and neglect the effect of chain length on the rate of mass transport from solution to the interface. When both species are present in solution at volume fractions of 10^{-4} , theoretical models predict that the longer chains will adsorb preferentially and almost completely exclude the shorter chains at equilibrium.⁶¹⁻⁶⁴ Immediately following the exposure of a clean surface to the bidisperse mixture, however, the shorter chains can adopt adsorbed configurations approximately 5 times more rapidly than the longer chains, based on the dynamic scaling of eq 12. The surface coverage of the shorter chains will then increase faster than the coverage of the longer chains. As a result, the surface coverage of the shorter chains may exceed its equilibrium value (which is very small) at short times. Overshoots may be then observed in the adsorbed amount of the short chains. In order to relax to equilibrium, the longer chains must then displace the shorter chains that adsorb initially, but competitive adsorption experiments show that the time required for displacement can be very large.^{7,8,64}

The behavior of diblock copolymers at low concentration should be contrasted with their behavior at higher concentrations. Although the present study shows that the nonadsorbing block in a diblock copolymer does not provide significant kinetic constraints at infinite dilution, other studies have shown that its effects become much more pronounced as the solution concentration and surface coverage increase.^{65,66} At higher concentrations, the nonadsorbing block of one chain may easily interfere with the adsorption of other chains, and the formation of block copolymer micelles adds further complications. As surface coverage increases, the diblock copolymers will form a polymer brush.^{67,68} In this case, Johner and Joanny⁶⁹ have predicted that the rate-limiting step in adsorption will be the passage of chains through the brush to the surface rather than the configurational relaxation that is treated by the simulations reported here. Long nonadsorbing blocks are expected to have a strong effect on the adsorption dynamics when brushes form, because the nonadsorbing block increases the free energy barrier that must be overcome to transfer a polymer chain from solution through the brush to the surface. Simulations of multichain block copolymer systems would be required to examine this issue quantitatively.

Finally, the scaling behavior given in eqs 15 and 16 for the adsorption dynamics of isolated random copolymers might motivate theoretical and experimental studies of their adsorption dynamics from concentrated solutions and melts. In particular, the relationship among the rich phase behavior of random copolymer melts,^{49,50} their adsorption dynamics, and the possibility of surface-induced phase segregation remains an interesting and largely unexplored question. Simulations of concentrated random copolymer systems with appropriate energetic parameters between A and B segments could be aimed in this direction.

References and Notes

- (1) Takahashi, A.; Kawaguchi, M. *Adv. Polym. Sci.* **1982**, *46*, 1.
- (2) Cohen-Stuart, M.; Cosgrove, T.; Vincent, B. *Adv. Colloid Interface Sci.* **1986**, *24*, 143.
- (3) de Gennes, P.-G. *Adv. Colloid Interface Sci.* **1987**, *27*, 189.
- (4) Sanchez, I. C. *Physics of Polymer Surfaces and Interfaces*; Butterworth-Heinemann: Boston, 1992.
- (5) Furusawa, K.; Yamamoto, K. *J. Colloid Interface Sci.* **1983**, *96*, 268.
- (6) Pefferkorn, E.; Haouam, A.; Varoqui, R. *Macromolecules* **1989**, *22*, 2677.
- (7) Johnson, H. E.; Granick, S. *Science* **1992**, *255*, 966.
- (8) Schneider, H. M.; Granick, S. *Macromolecules* **1992**, *25*, 5054.
- (9) Fu, T. Z.; Stimming, U.; Durning, C. J. *Macromolecules* **1993**, *26*, 3271.
- (10) Kremer, K. *J. Phys. (Paris)* **1986**, *47*, 1269.
- (11) (a) Barford, W.; Ball, R. C.; Nex, C. M. M. *J. Chem. Soc., Faraday Trans. 1* **1986**, *82*, 3233. (b) Barford, W.; Ball, R. C. *J. Chem. Soc., Faraday Trans. 1* **1987**, *83*, 2515.
- (12) Chakraborty, A. K.; Shaffer, J. S.; Adriani, P. M. *Macromolecules* **1991**, *24*, 5226.
- (13) Chakraborty, A. K.; Adriani, P. M. *Macromolecules* **1992**, *25*, 2470.
- (14) Shaffer, J. S.; Chakraborty, A. K. *Macromolecules* **1993**, *26*, 1120.
- (15) Adriani, P. M.; Chakraborty, A. K. *J. Chem. Phys.* **1993**, *98*, 4263.
- (16) de Gennes, P.-G. In *Molecular Conformation and Dynamics of Macromolecules in Condensed Systems*; Nagasawa, M., Ed.; Elsevier: New York, 1988.
- (17) McCrackin, F. L. *J. Chem. Phys.* **1967**, *47*, 1980.
- (18) Eisenriegler, E.; Kremer, K.; Binder, K. *J. Chem. Phys.* **1982**, *77*, 6296.
- (19) (a) Livne, S.; Meirovitch, H. *J. Chem. Phys.* **1988**, *88*, 4498. (b) Meirovitch, H.; Livne, S. *J. Chem. Phys.* **1988**, *88*, 4507.
- (20) Bishop, M.; Clarke, J. H. R. *J. Chem. Phys.* **1990**, *93*, 1455.
- (21) Rubin, R. J. *J. Chem. Phys.* **1965**, *43*, 2392.
- (22) Wiegel, F. In *Phase Transitions and Critical Phenomena*; Domb, C., Green, M. S., Eds.; Academic Press: New York, 1983; Vol. 7.
- (23) Marques, C. M.; Joanny, J. F. *Macromolecules* **1990**, *23*, 268.
- (24) Balazs, A. C.; Gempe, M.; Lantman, C. M. *Macromolecules* **1991**, *24*, 168.
- (25) Clancy, T. C.; Webber, S. E. *Macromolecules* **1993**, *26*, 628.
- (26) Poland, D. *Macromolecules* **1991**, *24*, 3361.
- (27) Hahn, T. D.; Kovac, J. *Macromolecules* **1990**, *23*, 5153.
- (28) Konstadinidis, K.; Prager, S.; Tirrell, M. *J. Chem. Phys.* **1992**, *97*, 7777.
- (29) Cosgrove, T.; Prestidge, C. A.; King, S. M.; Vincent, B. *Langmuir* **1992**, *8*, 2206.
- (30) King, S. M.; Cosgrove, T. *Macromolecules* **1993**, *26*, 5414.
- (31) Brand, J. L.; Arena, M. V.; Deckert, A. A.; George, S. M. *J. Chem. Phys.* **1990**, *92*, 5136.
- (32) Silverberg, M. *J. Chem. Phys.* **1993**, *99*, 9255.
- (33) Huang, D.; Fichthorn, K. A., personal communication.
- (34) Kremer, K.; Binder, K. *Comput. Phys. Rep.* **1988**, *7*, 259.
- (35) Deutsch, H. P.; Binder, K. *J. Chem. Phys.* **1991**, *94*, 2294.
- (36) Carmesin, I.; Kremer, K. *Macromolecules* **1988**, *21*, 2819.
- (37) The term "segment" is used here to denote one repeat unit of the lattice polymer as it is represented in the BFM. Two segments of the lattice polymer and the bond that joins them can be mapped approximately to one Kuhn segment of a real polymer.
- (38) Doi, M.; Edwards, S. F. *The Theory of Polymer Dynamics*; Oxford University Press: New York, 1986.
- (39) Paul, W.; Binder, K.; Heermann, D. W.; Kremer, K. *J. Phys. (Paris) II* **1991**, *1*, 1395; *J. Non-Cryst. Solids* **1991**, *131-133*, 650.
- (40) Wittmer, J.; Paul, W.; Binder, K. *Macromolecules* **1992**, *25*, 7211.
- (41) Wittmann, H.-P.; Kremer, K.; Binder, K. *J. Chem. Phys.* **1992**, *96*, 6291.
- (42) Madras, N.; Sokal, A. D. *J. Stat. Phys.* **1987**, *47*, 573.
- (43) Hilhorst, H. J.; Deutch, J. M. *J. Chem. Phys.* **1975**, *63*, 5153.
- (44) Boots, H.; Deutch, J. M. *J. Chem. Phys.* **1977**, *67*, 4608.
- (45) Le Guillou, J. C.; Zinn-Justin, J. *Phys. Rev. Lett.* **1977**, *39*, 95.
- (46) Attempted moves from $z = 1$ to $z = 2$ are subject to the activation barrier E_z , while attempted moves from $z = 2$ to $z = 1$ are not activated. Detailed balance then dictates that E_z is the energy difference between lattice planes $z = 1$ and $z = 2$.
- (47) All x and y coordinate locations are energetically equivalent, because both positive and negative displacements in the x and y directions are subject to the activation barrier for surface diffusion.
- (48) Bates, F. S.; Fredrickson, G. H. *Annu. Rev. Phys. Chem.* **1990**, *41*, 525.
- (49) Shakhnovich, E. I.; Gutin, A. M. *J. Phys. (Paris)* **1989**, *50*, 1843.
- (50) Fredrickson, G. H.; Milner, S. T. *Phys. Rev. Lett.* **1991**, *67*, 835.
- (51) Consider, for example, a situation in which only one segment is in contact with the surface, and that segment is the j th segment along the chain. If $j \leq N_A$, then the adsorbing block is assigned to segments 1 through N_A ; if $j > N_A$, then the adsorbing block is assigned to segments $N - N_A + 1$ through N .
- (52) In other words, the scaling behavior of the relaxation time τ , defined by eq 10, should be universal and therefore independent of the molecular model used for its calculation.
- (53) The error estimates are reported as 95% confidence intervals for the parameters that are obtained from nonlinear least-squares regression to the power law functional form. The error estimates account for the statistical uncertainty in the values of the relaxation times as well as the quality of the fit to the power law form itself. See: Press, W. H.; Flannery, B. P.; Teukolsky, S. A.; Vetterling, W. *Numerical Recipes*; Cambridge University Press: Cambridge, U.K., 1986.
- (54) The precise values of the scaling law exponents may change slightly if data points over a wider range of chain lengths are used in the power law fitting. Computational limitations prevent the extension of the range of chain lengths that is used to extract the scaling exponents.
- (55) The incorrect scaling argument proceeds as follows: When the first segment makes contact with the surface at the start of the adsorption process, the chain center of mass is approximately one radius of gyration, R_g , from the surface plane. When the adsorption is complete, the chain lies almost flat on the surface, and its center of mass nearly coincides with the surface plane. If τ_{HP} is estimated as the time required for the chain center of mass to diffuse a distance equal to R_g , then one obtains $\tau_{HP} \approx R_g^2/6D \sim N^{2\nu}/N^{-1} \sim N^{1+2\nu}$. (Rouse scaling for D is used rather than Zimm scaling because hydrodynamic interactions are not incorporated in the present model.) Using the values of ν for three dimensions, this simple scaling argument predicts $\alpha = 2$ for phantom chains and $\alpha \approx 2.18$ for self-avoiding chains.
- (56) Another way of stating this is that a lattice model cannot faithfully represent structural features of real polymers that would be mapped onto a lattice length scale approaching one lattice unit.
- (57) Kurata, M.; Yamakawa, H.; Teramoto, E. *J. Chem. Phys.* **1958**, *28*, 785.
- (58) Wall, F. T.; Erpenbeck, J. J. *J. Chem. Phys.* **1959**, *30*, 634.
- (59) Matsushita, Y.; Noda, I.; Nagasawa, M.; Lodge, T. P.; Amis, E. J.; Han, C. C. *Macromolecules* **1984**, *17*, 1785.
- (60) We thank a reviewer for suggesting this explanation.
- (61) Roe, R. J. *J. Chem. Phys.* **1974**, *60*, 4192.
- (62) Cohen-Stuart, M. A.; Scheutjens, J. M. H. M.; Fleer, G. J. *J. Polym. Sci., Polym. Phys. Ed.* **1980**, *18*, 559.
- (63) Scheutjens, J. M. H. M.; Fleer, G. J. In *The Effect of Polymers on Dispersion Properties*; Tadros, Th. F., Ed.; Academic Press: New York, 1982.
- (64) Kawaguchi, M. *Adv. Colloid Interface Sci.* **1990**, *32*, 1. See especially Figure 5 of this reference.
- (65) Leermakers, F. A. M.; Gast, A. P. *Macromolecules* **1991**, *24*, 718.
- (66) Motschmann, H.; Stamm, M.; Toprakcioglu, Ch. *Macromolecules* **1991**, *24*, 3681.
- (67) Milner, S. T. *Science* **1991**, *251*, 905.
- (68) Halperin, A.; Tirrell, M.; Lodge, T. P. *Adv. Polym. Sci.* **1991**, *100*, 31.
- (69) Johnner, A.; Joanny, J. F. *Macromolecules* **1990**, *23*, 5299.